

# Rate-Diverse Gaussian Multiple Access: Efficient Encoder and Decoder Designs

Pingping Chen, *Member, IEEE*, Long Shi, *Member, IEEE*, Yi Fang, *Member, IEEE*, Francis C. M. Lau, *Senior Member, IEEE*, and Jun Cheng, *Member, IEEE*

**Abstract**—In this work, we develop a pair of rate-diverse encoder and decoder for a two-user Gaussian multiple access channel (GMAC). The proposed scheme enables the users to transmit with the same codeword length but different coding rates under diverse user channel conditions. First, we propose the row-combining (RC) method and row-extending (RE) method to design practical low-density parity-check (LDPC) channel codes for rate-diverse GMAC. Second, we develop an iterative rate-diverse joint user messages decoding (RDJD) algorithm for GMAC, where all user messages are decoded with a single parity-check matrix. In contrast to the conventional network-coded multiple access (NCMA) and compute-forward multiple access (CFMA) schemes that first recover a linear combination of the transmitted codewords and then decode both user messages, this work can decode both the user messages simultaneously. Extrinsic information transfer (EXIT) chart analysis and simulation results indicate that RDJD can achieve gains up to 1.0 dB over NCMA and CFMA in the two-user GMAC. In particular, we show that there exists an optimal rate allocation for the two users to achieve the best decoding performance given the channel conditions and sum rate.

**Index Terms**—Gaussian multiple access channel (GMAC), low-density parity-check (LDPC) code, extrinsic information transfer (EXIT) chart analysis.

## I. INTRODUCTION

An interference channel has been considered as a canonical model to understand the design principles of cellular networks with inter-cell interference [1]. A Gaussian multiple access channel (GMAC) is a simple interference channel where two users communicate with one receiver in the presence of additive white Gaussian noise (AWGN). The capacity region of the two-user GMAC has been characterized in [2], [3], where the corner points of the capacity region can be achieved via single user decoding, and the points in between can be achieved by time sharing. It is also shown that any rate pair in the capacity region can be attained by rate splitting or joint decoding without time sharing [4], [5]. Some enabling solutions of GMAC have been extensively studied in the field of coding and information theory, such as superposition coding

[6], [7], successive interference cancellation (SIC), and the message passing algorithm (MPA) [8], [9]. As the best known achievable strategy, Han-Kobayashi scheme is a joint unique decoding of messages for the two-user interference channel [10]. Each user splits the information into private and common parts by superposition encoding. Both parts are optimally recovered by using simultaneous joint decoding [11], [12]. Since the recovery of the private part can be simply decoded as in the point-to-point communications, the main challenge lies in the transmission and recovery of the common messages, where each receiver treats the interference channel as a MAC.

For a GMAC, multiple users transmit their messages simultaneously to a receiver. Among the various types of receivers, SIC has been widely studied because of its simplicity, where serial decision and cancellation are performed [13]–[16]. In a SIC-aided GMAC, the received signal powers from different users at the receiver are significantly different. Thus, the receiver first decodes the message corresponding to the strongest signal and removes this message from its observation. The corner points of the two-user capacity can be achieved by SIC in GMAC, while other points can be achieved by time-sharing, rate-splitting, or joint decoding. In particular, capacity-approaching low-density parity-check (LDPC) codes have been designed for two-user GMAC by using joint decoders at the receiver [17]–[19]. A more recent study has optimized the power ratio of the two users to minimize the required SNR for a given rate under the joint decoding in a GMAC [20].

Not until very recently has the notion of physical-layer network coding (PNC) been adopted into the two-user GMAC, referred to as network-coded multiple-access (NCMA) [21]. The core of PNC is to turn mutual interference between signals received from simultaneously transmitting users into useful network-coded (NC) messages [22], [23]. As a prevailing decoding in PNC, XOR-based channel decoding (XOR-CD) aims to decode bitwise NC messages of user messages. The first work on NCMA has used XOR-CD and multiuser decoding (MUD) to first decode the NC message and then both user messages [21]. Later, to achieve a high-efficient transmission, a NCMA system that operates with high-order modulations of QPSK and 16-QAM has been developed [24]. To exploit different channel conditions, different modulations for distinct users have been adopted to realize modulation-diverse NCMA with the same coding rate [25]. It was shown that the system throughput of NCMA with BPSK+QPSK outperforms those of modulation-homogeneous NCMA. More recently, a NCMA downlink system for unmanned aerial vehicle (UAV) communications has been developed to improve system throughput

P. Chen is with the School of Physics and Information Engineering, Fuzhou University, Fujian 350002, China (e-mail: ppchen.xm@gmail.com).

L. Shi is with the Department of Electronic and Optical Engineering, Nanjing University of Science and Technology, Nanjing 210094, China (slong1007@gmail.com).

Y. Fang is with the School of Information Engineering, Guangdong University of Technology, Guangzhou 510006, China (e-mail: fangyi@gdut.edu.cn).

F. C. M. Lau is with the Department of Electronic and Information Engineering, Hong Kong Polytechnic University, Kowloon, Hong Kong (e-mail: franciscm.lau@polyu.edu.hk).

Jun Cheng is with the Department of Intelligent Information Engineering and Science, Doshisha University, Kyoto 610-0321, Japan (e-mail: jcheng@ieee.org).

by NCMA-based superposition coding [26].

In another line of PNC-based GMAC, compute-and-forward multiple access (CFMA) generalizes PNC to multi-user networks by utilizing structured nested lattice codes [27], [28]. The authors have extended compute-and-forward to a GMAC from a theoretical perspective [29]. By appropriately scaling the lattice codes, it can attain the dominant face of the capacity region of GMAC with a single-user decoder without time sharing. Following this study, practical off-the-shelf LDPC codes and efficient decoding algorithms have been adopted for CFMA [32]. Similar to NCMA, CFMA first decodes a linear NC combination of two codewords by XOR-CD, and then recovers the individual user codewords. It has been shown that CFMA can achieve some rate pairs on the dominant face of the capacity region, whereas the conventional SIC fails to attain these rate pairs. However, the achievable rate of XOR-CD in a two-user GMAC is limited by the worse user channel even when the other channel is error-free. In this context, CFMA may not perform well over the user channels that are significantly diverse. This is due to the fact that CFMA decodes the NC message by using the parity-check matrix of the better user channel only.

In this paper, we propose a two-user uplink rate-diverse GMAC over diverse channel conditions. We call the user with the better channel condition as the strong user and that with the worse channel as the weak user. The proposed system allows the users to adopt different channel codes, i.e., a low-rate code for the weak user and a high-rate code for the strong user. This work is primarily motivated by the observation that the achievable rate of XOR-CD in a two-user GMAC is limited by the worse user channel even though the other channel is error-free, and this limitation prevents the strong user from fully exploiting its superior channel condition. In this context, the goal of this paper lies in the encoder and decoder designs that can fully exploit the diverse channel conditions in a two-user GMAC. Our main contributions are as follows.

- 1) For the encoder of the proposed scheme, we design practical LDPC codes for different users by two methods, i.e., row-combining (RC) method and row-extending (RE) method. The core of these methods is that the two channel codes share a common parity-check matrix with a high code rate. In particular, the parity-check matrix of the low-rate code owns a residual matrix alongside with the common matrix, and the parity-check matrix of the high-rate code is embedded in that of the low-rate code.
- 2) For the decoder of the proposed scheme, we propose an iterative rate-diverse joint user-message decoding (RDJD) algorithm to decode user messages within the low-rate parity-check matrix. The proposed decoder consists of a joint user channel decoder (JUD) to decode the joint user message and a residual user decoder (RUD) to decode the individual user messages. It differs from NCMA and CFMA which first decode the NC message and then recover both user messages based on the decoded NC messages.
- 3) We investigate the error performance of the iterative RDJD using an extrinsic information transfer (EXIT) chart. Analytical results show that iterative decoding

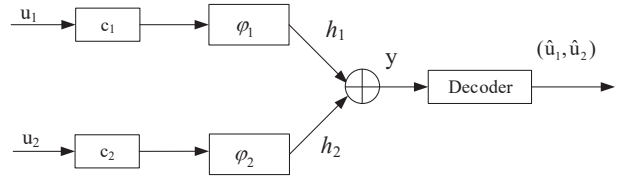


Fig. 1. GMAC channel model.

between JUD and RUD provides large gains over the non-iterative one. Our simulations further demonstrate that iterative RDJD achieves significant performance gains over NCMA and CFMA. This gain can be up to 1 dB when the user channels are largely different. In particular, both analytical and simulation results indicate that there exists an optimal rate pair for the two users to achieve the best performance under given channel conditions. Moreover, we show that the proposed RDJD can approach the rate pair on the dominant face of the capacity region without rate-splitting or time-sharing.

The remainder of this paper is organized as follows. Section II presents the related background for GMAC. Section III puts forth the concept of rate-diverse GMAC and elaborates its encoder and decoder. Section IV investigates the iterative decoding of the proposed scheme by means of an EXIT chart analysis. Section V presents the performance of the rate-diverse GMAC and validates its advantages. Finally, Section VI concludes the paper.

## II. RELATED BACKGROUND

In this paper, we use a boldface letter to denote a vector and the corresponding italic letter to denote a symbol within the vector. For example,  $\mathbf{x}$  is a vector, and  $x$  is a symbol within the vector.

### A. System Model

We consider the two-user GMAC in Fig. 1. Let  $\mathbb{F}_q$  denote a  $q$ -ary finite field and  $q$  is a prime power. Let  $\mathbf{u}_1$  and  $\mathbf{u}_2$  be two source message vectors of lengths  $K_1$  and  $K_2$  for users 1 and 2, respectively,  $u_1, u_2 \in \mathbb{F}_q$ . Channel codes are used to encode  $\mathbf{u}_1$  and  $\mathbf{u}_2$  into two length- $L$  vectors  $\mathbf{c}_1$  and  $\mathbf{c}_2$  with rates of  $R_1 = K_1/L$  and  $R_2 = K_2/L$ , respectively, where  $c_1, c_2 \in \mathbb{F}_q$ . The channel codes with  $R_1$  and  $R_2$  have parity-check matrices  $\mathbf{H}_1$  and  $\mathbf{H}_2$ , respectively. We use  $\Gamma_1$  and  $\Gamma_2$  to denote the channel coding for the two users, i.e.,

$$\mathbf{c}_1 = \Gamma_1(\mathbf{u}_1), \mathbf{c}_2 = \Gamma_2(\mathbf{u}_2). \quad (1)$$

Users 1 and 2 generate two signal vectors  $\mathbf{x}_1$  and  $\mathbf{x}_2$  by symbol-wise modulations, i.e.,  $x_1 = \varphi_1(c_1)$  and  $x_2 = \varphi_2(c_2)$ , where  $\varphi_m$  defines the modulation from  $c_m$  to  $x_m$  of user  $m$ . Let  $\chi_m$  denote the constellation set of user  $m$ . The cardinality of  $\chi_m$  is  $q$ , i.e.,  $|\chi_m| = q$  (by cardinality, we mean the number of distinct elements in the set), and  $x_m \in \chi_m$ ,  $m = 1, 2$ .

Let  $h_1$  and  $h_2$  denote the channel coefficients from user 1 and user 2 to the receiver, respectively. Assuming perfect

synchronization between the two users, the signal at the receiver is given by

$$\mathbf{y} = h_1 \mathbf{x}_1 + h_2 \mathbf{x}_2 + \mathbf{z}, \quad (2)$$

where the vector  $\mathbf{z}$  contains white Gaussian noise samples with zero mean and variance  $N_0/2$ . Without loss of generality, we assume that  $|h_1| \geq |h_2|$  and  $R_1 \geq R_2$  in this paper.

With respect to (2), let  $x = h_1 x_1 + h_2 x_2$  denote a superimposed symbol under channel coefficients  $h_1$  and  $h_2$  (i.e., the noise-free received signal). We define the set that collects all superimposed symbols under  $h_1$  and  $h_2$  as  $\tilde{\chi} = \{h_1 x_1 + h_2 x_2 | x_1 \in \chi_1, x_2 \in \chi_2\}$ . In addition, we denote  $\mathbf{x}$  as a vector of the superimposed symbols,  $\mathbf{x}(i) \in \tilde{\chi}$ ,  $i = 1, 2, \dots, L$ . We consider block fading channels where  $h_1$  and  $h_2$  keep unchanged during one block transmission and vary from one block to the next. In general,  $|\tilde{\chi}| = q^2$ . We then define a pair of coded messages  $(c_1, c_2)$  as a joint message. The set of joint messages is given by

$$\mathcal{C} = \{(c_1, c_2) | c_1, c_2 \in \mathbb{F}_q\}, \quad (3)$$

where  $|\mathcal{C}| = q^2$ . Accordingly, each element in  $\tilde{\chi}$  is associated with a joint message  $(c_1, c_2)$  in  $\mathcal{C}$ . Thus,  $\mathcal{C} \rightarrow \tilde{\chi}$  is a one-to-one mapping under given fading channel coefficients. The receiver in GMAC aims to recover all user messages from the received signal  $\mathbf{y}$ .

### B. Problem at a Glance

The capacity region of a two-user GMAC is given by the convex hull of the set of rate pairs  $(R_1; R_2)$  that satisfies [36]

$$\begin{aligned} R_1 &< I(x_1; y|x_2) \\ R_2 &< I(x_2; y|x_1) \\ R_1 + R_2 &< I(x_1, x_2; y), \end{aligned} \quad (4)$$

for some joint distribution  $(x_1; x_2) \sim p(x_1)p(x_2)$ . The SIC decoding can achieve one of the two corner points of the pentagonal region [36]

$$\begin{aligned} R_1 &< I(x_1; y), \\ R_2 &< I(x_2; y|x_1). \end{aligned} \quad (5)$$

The remaining points on the dominant face can be achieved by time-sharing and rate-splitting [36]. Every rate pair in the interior of the rate region can be achieved by simultaneous decoding. Assuming that the messages are drawn uniformly at random, the average probability of error is defined as

$$P_e^{(n)} = P\{(\hat{u}_1, \hat{u}_2) \neq (u_1, u_2)\}. \quad (6)$$

A rate pair  $(R_1; R_2)$  is said to be achievable if there exists a sequence of  $(2^{nR_1}, 2^{nR_2}; n)$  codes such that  $\lim_{n \rightarrow \infty} P_e^{(n)} = 0$ .

CFMA has been proposed to achieve some rate pairs of GMAC capacity without rate-splitting or time sharing [27], [29]. The scheme employs nested lattice codes and a sequential decoding scheme. In the first step, the receiver decodes a linear combination of codewords  $a_1 \mathbf{u}_1 + a_2 \mathbf{u}_2$  (modulo-lattice reduced) with non-zero integer coefficients  $a_1$  and  $a_2$ ; in the second step, the receiver exploits this linear combination as side information to decode one of the codewords (either  $\mathbf{u}_1$

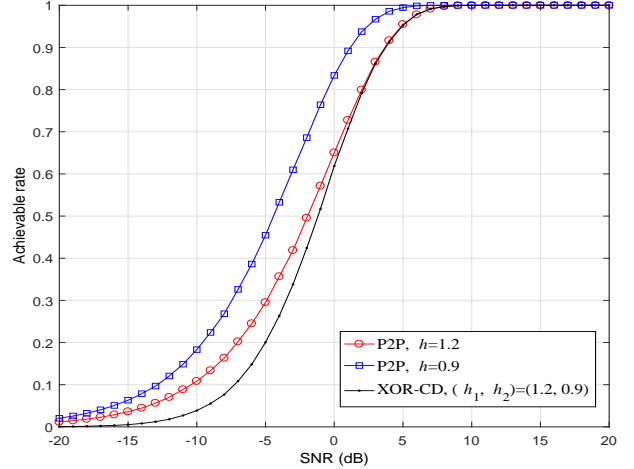


Fig. 2. Achievable rates of XOR-CD with  $(h_1, h_2) = (1.2, 0.9)$ .

or  $\mathbf{u}_2$ ); finally, the receiver recovers the other message from the outputs of previous two steps. Furthermore, this decoding scheme achieves (a part of) the dominant face of the capacity region for the GMAC [30]. Later on, rather than based on lattice codes, a generalization of CFMA based on nested linear codes and joint typicality encoding and decoding is presented [31].

In the linear-code-based GMAC, the linear-network coding  $\phi$  mapping from a superimposed vector  $\mathbf{x}$  to a NC message vector  $\mathbf{c}$  is defined as

$$\begin{aligned} \mathbf{c} &= \phi(\mathbf{x}) = \phi(h_1 \mathbf{x}_1 + h_2 \mathbf{x}_2) = a_1 \mathbf{c}_1 + a_2 \mathbf{c}_2 \\ &= a_1 \varphi_1^{-1}(\mathbf{x}_1) \oplus_q a_2 \varphi_2^{-1}(\mathbf{x}_2), \end{aligned} \quad (7)$$

where  $a_1, a_2 \in \mathbb{F}_q$ ,  $\oplus_q$  denotes the addition over  $\mathbb{F}_q$ , and  $\varphi_m^{-1}$  denotes the inverse of  $\varphi_m$ ,  $m = 1, 2$ .

The following theorem describes an achievable rate region with CFMA.

*Theorem 1* [31]: A rate pair  $(R_1, R_2)$  is achievable with nested linear codes and under CFMA decoding if for some non-zero coefficient vector  $(a_1, a_2) \in \mathbb{F}_q^2$  and for some mapping  $\varphi_1^{-1}$  and  $\varphi_2^{-1}$ , we have either

$$\begin{aligned} R_1 &< H(x_1) - \max\{H(c|y), H(x_1, x_2|y, c)\}, \\ R_2 &< H(x_1) - H(c|y), \end{aligned} \quad (8)$$

or

$$\begin{aligned} R_1 &< H(x_1) - H(c|y), \\ R_2 &< H(x_2) - \max\{H(c|y), H(x_1, x_2|y, c)\}, \end{aligned} \quad (9)$$

where

$$\begin{aligned} c &= a_1 c_1 \oplus_q a_2 c_2, \\ (c_1, c_2) &= (\varphi_1^{-1}(x_1), \varphi_2^{-1}(x_2)), \end{aligned} \quad (10)$$

and

$$H(c|y) = H(c) - I(c; y). \quad (11)$$

By Theorem 1, for some  $(a_1, a_2) \in \mathbb{F}_q^2$ , CFMA can achieve non-corner rate points in (8) and (9), which are distinct from corner points on the dominant face.

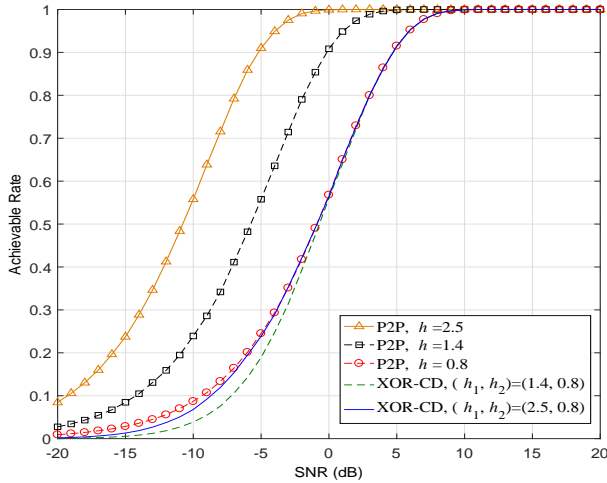


Fig. 3. Achievable rates of XOR-CD with  $(h_1, h_2) = (1.4, 0.8)$  and  $(h_1, h_2) = (2.5, 0.8)$ , respectively.

It can be seen from (8)-(11) that the rate  $I(c; y)$  is vital in the achievable rate pairs. In the following, we illustrate  $I(c; y)$  in CFMA over different channel gains  $h_1$  and  $h_2$ . We will show that the achievable rate  $I(c; y)$  is strictly limited by the worse channel of the two user channels, even though the other user channel is sufficiently good. We consider a binary channel-coded two-user CFMA, i.e.,  $q = 2$ . In this case, XOR-CD is used in CFMA to decode the NC message vector  $\mathbf{c} = \mathbf{c}_1 \oplus \mathbf{c}_2$  with  $a_1 = a_2 = 1$  in (7). Fig. 2 shows the achievable rate  $I(c; y)$  of XOR-CD. The achievable rate of point-to-point (P2P) communication with a channel gain  $h$  is also plotted as an upper bound. We can see that XOR-CD with  $(h_1, h_2) = (1.2, 0.9)$  has a rate loss as compared with P2P with  $h = 0.9$  in the low-to-medium SNR regimes, and approaches the latter one in the high SNR regime. This rate loss is increased up to 3–5 dB as compared to P2P channel with  $h = 1.2$  over all SNR regimes.

We enlarge the difference of the two channel conditions and plot the results in Fig. 3. First, it shows that XOR-CD with  $(h_1, h_2) = (1.4, 0.8)$  has a slight rate loss as compared with P2P with  $h = 0.8$ , and the rate loss is increased to about 4–6 dB with  $h = 1.4$ . Second, we note that XOR-CD with  $(h_1, h_2) = (1.4, 0.8)$  performs close to XOR-CD even with a much larger  $h_1$ , e.g.,  $(h_1, h_2) = (2.5, 0.8)$ . From these results, one can deduce that

$$I(c; y) \leq \min(C_1, C_2), \quad (12)$$

where  $C_1$  and  $C_2$  denote the channel capacities of the users 1 and 2, respectively. Thus,  $I(c; y)$  has a rate loss compared to the capacity of the better channel, and the loss becomes larger as the channel difference becomes more significant. Moreover, the performance loss of XOR-CD degrades the decoding performance of CFMA and NCMA, as the second step for these two schemes is to decode both user messages. The simulation results in [25] have also shown that the uplink with the poorest channel condition becomes the bottleneck of NCMA, when all users use the same modulation and code rate by ignoring their individual channel gains.

### III. PROPOSED CHANNEL CODE AND DECODER DESIGNS

This section develops a pair of encoder and decoder for a two-user GMAC to employ different coding rates according to the channel conditions. First, we develop the channel codes by the RE and RC methods. Second, we propose a novel RDJD decoder to directly decode both user messages rather than to decode the users' messages one by one, as in CFMA and NCMA.

#### A. Proposed Channel Code Designs

We suppose that users 1 and 2 are the strong and weak users, respectively. We design two codes for the two users with the same codeword length but different code rates. We consider that user 1 adopts a code  $\mathcal{C}_1$  of rate  $R_1$  with a parity-check matrix  $\mathbf{H}_1$ , while user 2 adopts a code  $\mathcal{C}_2$  of rate  $R_2$  with a parity-check matrix  $\mathbf{H}_2$ . Note that  $R_1 \geq R_2$ . Moreover, we design the codes that satisfy  $\mathcal{C}_1 \supseteq \mathcal{C}_2$ . That is, the code  $\mathcal{C}_2$  is a subcode of  $\mathcal{C}_1$  given the same codeword length. In this way, the user messages can be decoded by a single decoder based on the low-rate parity-check matrix. To this end, we propose the RE and RC channel code design methods as follows.

1) *RE method*: Given the parity-check matrix  $\mathbf{H}_1$  of user 1, we construct the parity-check matrix  $\mathbf{H}_2$  for  $\mathcal{C}_2$  of user 2 with the lower rate  $R_2$  by appending an additional matrix  $\mathbf{H}_e$  below in  $\mathbf{H}_1$ , as shown in (13). To reduce performance loss, it is required that the newly added rows in  $\mathbf{H}_e$  cannot introduce cycle-4 in  $\mathbf{H}_2$ .

$$\mathbf{H}_2 = \left( \begin{array}{c} \mathbf{H}_1 \\ \hline \begin{array}{cccccccc} 1 & 1 & 0 & 0 & \cdots & 0 & 1 & 0 & 1 \\ \vdots & \vdots & \vdots & \vdots & \vdots & \vdots & \vdots & \vdots & \vdots \end{array} \end{array} \right) \Bigg\} \mathbf{H}_e. \quad (13)$$

2) *RC method*: Given  $\mathbf{H}_2$  of rate  $R_2$ , we first select some rows out of  $\mathbf{H}_2$  to form a matrix  $\mathbf{H}_r$ ; the matrix formed by the remaining rows in  $\mathbf{H}_2$  is denoted by  $\mathbf{H}_d$ , as shown in (14a). Second, every  $\lambda$  rows in  $\mathbf{H}_r$  are grouped to generate a new row under some finite-field operations, and the resulting matrix  $\overline{\mathbf{H}}_r$  consisting of the new rows has fewer rows than  $\mathbf{H}_r$ . Finally, as shown in (14b), we construct a new matrix  $\mathbf{H}_1 = [\mathbf{H}_d; \overline{\mathbf{H}}_r]$  as the parity-check matrix for user 1 with rate  $R_1$ . Obviously,  $\mathbf{H}_1$  has fewer rows than  $\mathbf{H}_2$ .

Note that we can combine the rows in  $\mathbf{H}_r$  in various ways, which may lead to different performance. For example, we can simply perform XOR on every  $\lambda = 2$  rows to generate  $\overline{\mathbf{H}}_r$ . We require that the rows to be combined cannot have two or more "1"s in the same column such that the variable-node





$o = \eta(\mathbf{c}_{1,2}(i)) = \eta([\mathbf{c}_1(i), \mathbf{c}_2(i)])$ . Then,  $o \in \Delta = \{0, 1, 2, 3\}$ . Conversely, we use  $\eta_m^{-1}(o)$  to denote the  $m$ th bit in the bit vector converted from  $o$ ,  $m = 1, 2$ <sup>1</sup>. Moreover, we denote  $p^o(i) = \Pr\{\mathbf{c}_{1,2}(i) = \eta^{-1}(o)\}$ .

Let a length-4 probability vector  $\mathbf{p}(i)$  denote the soft message of  $\mathbf{c}_{1,2}(i)$  passing within JUD. We perform sum-product algorithm (SPA) within  $\mathbf{H}_c$  that consists of two sets of nodes, i.e., variable nodes  $\mathbf{v}$  and check nodes  $\mathbf{t}$ . A variable node  $\mathbf{v}(i)$  corresponds to  $\mathbf{c}_{1,2}(i)$ .

• *Initial messages for JUD.* Recall that the superimposed symbol  $x = h_1x_1 + h_2x_2$  has four possible values,  $x \in \tilde{\chi} = \{h_1 + h_2, h_1 - h_2, -h_1 + h_2, -h_1 - h_2, \}$  and  $\tilde{\chi}^j$  is the  $j$ th element in  $\tilde{\chi}$  for each received signal. We introduce a length-4 channel probability vector  $\mathbf{p}_{ch}(i)$  for the  $i$ th variable node, where the  $j$ th element  $\mathbf{p}_{ch}^j(i)$  denotes the probability of  $\mathbf{x}(i) = \tilde{\chi}^j$  and is computed by

$$\begin{aligned} \mathbf{p}_{ch}^j(i) &= \Pr(\mathbf{y}(i)|\mathbf{x}(i) = \tilde{\chi}^j, h_1, h_2) \\ &= \frac{1}{\beta\pi\sigma^2} \exp\left(-\frac{|\mathbf{y}(i) - \tilde{\chi}^j|^2}{2\sigma^2}\right), \end{aligned} \quad (19)$$

where  $\beta$  is a normalization factor that ensures  $\sum_{j=0}^3 \mathbf{p}_{ch}^j(i) = 1$ .

In addition, JUD has *a priori* information which is the extrinsic soft information  $\mathbf{e}^j(i)$  of user 2 coming from RUD, and  $\mathbf{e}^j(i)$  denotes the probability of  $\mathbf{c}_2(i) = j$ ,  $j \in \{0, 1\}$ . Then, the initial information for JUD can be computed by

$$\mathbf{p}^o(i) = \beta \mathbf{p}_{ch}^o(i) \mathbf{e}^j(i), \quad j = \eta_2^{-1}(o), \quad o \in \Delta. \quad (20)$$

Note that  $[\mathbf{e}^0(i) \ \mathbf{e}^1(i)] = [0.5, 0.5]$  in the first outer iteration for all the bits.

• *Message update of variable nodes and check nodes.* We use functions VAR and CHK to represent message updating at the variable nodes and check nodes, respectively. The explicit update rules of VAR and CHK with degree three are given in Appendix A. The messages from the variable nodes with degree greater than three can be recursively calculated by

$$\begin{aligned} \mathbf{v}_{\rightarrow k} &= \text{VAR}(\mathbf{p}(1), \dots, \mathbf{p}(k-1), \mathbf{p}(k+1), \dots, \mathbf{p}(g)) \\ &= \text{VAR}(\mathbf{p}(g), \text{VAR}(\mathbf{p}(1), \dots, \mathbf{p}(k-1), \\ &\quad \mathbf{p}(k+1), \dots, \mathbf{p}(g-1))), \end{aligned} \quad (21)$$

where  $\mathbf{v}$  is a degree- $g$  variable node,  $\mathbf{v}_{\rightarrow k}$  denotes the messages from  $\mathbf{v}$  to its  $k$ th connected check node, and  $\mathbf{p}(k)$  denotes the input messages of  $\mathbf{v}$ ,  $k = 1, 2, \dots, g$ .

Similarly, the messages from the check nodes with degree greater than three are calculated by

$$\begin{aligned} \mathbf{t}_{\rightarrow k} &= \text{CHK}(\mathbf{q}(1), \dots, \mathbf{q}(k-1), \mathbf{q}(k+1), \dots, \mathbf{q}(d)) \\ &= \text{CHK}(\mathbf{q}(d), \text{CHK}(\mathbf{q}(1), \dots, \\ &\quad \mathbf{q}(k-1), \mathbf{q}(k+1), \dots, \mathbf{q}(d-1))), \end{aligned} \quad (22)$$

where  $\mathbf{t}$  is a degree- $d$  check node,  $\mathbf{t}_{\rightarrow k}$  denotes the message from  $\mathbf{t}$  to its  $k$ th connected variable node, and  $\mathbf{q}(k)$  denotes the input messages of  $\mathbf{t}$ ,  $k = 1, 2, \dots, d$ .

• *Mapping of joint user messages.* After iterations,  $\mathbf{v}(i)$  is estimated as  $o \in \Delta$ . The *a-posteriori* probability of  $\mathbf{v}(i)$ ,

<sup>1</sup>For example, if  $\mathbf{c}_{1,2}(i) = [1 \ 0]$ , then  $o = \eta([1 \ 0]) = 2$ . Conversely,  $\eta_2^{-1}(2) = 0$ .

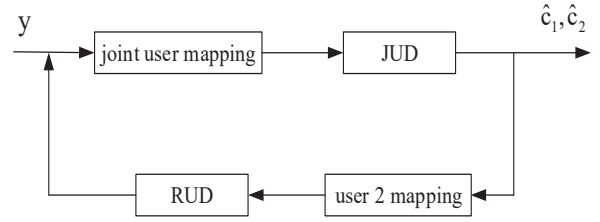


Fig. 5. Decoding diagram of RDJD.

denoted by  $\mathbf{w}(i) = [w^0(i), w^1(i), w^2(i), w^3(i)]$ , is evaluated in (22) by computing all incoming messages from the check nodes as well as the initial message. Finally, the joint user messages are decoded as

$$\begin{aligned} \mathbf{v}(i) &= \eta^{-1}(o) = [\mathbf{c}_1(i), \mathbf{c}_2(i)], \\ &\text{if } \underset{\forall j \in \Delta}{\text{argmax}} w^j(i) = o. \end{aligned} \quad (23)$$

2) *RUD:* The information  $\mathbf{w}$  is then passed into RUD, which picks up the *a priori* probability of  $\mathbf{c}_2$ . Let  $\mathbf{a}(i) = [\mathbf{a}^0(i), \mathbf{a}^1(i)]$  with  $\mathbf{a}^j(i)$  being the probability of  $\mathbf{c}_2(i) = j$ , which can be computed by

$$\mathbf{a}^j(i) = \sum_{\substack{\eta_2^{-1}(o)=j, \\ o \in \Delta}} w^o(i), \quad i = 1, 2, \dots, L. \quad (24)$$

With  $\mathbf{a}(i)$  as the *a priori* probability,  $i = 1, 2, \dots, L$ , we perform SPA decoder for the bit-wise estimation of  $\mathbf{c}_2$  within  $\mathbf{H}_a$ . After decoding, we generate extrinsic information  $\mathbf{e}^0$  and  $\mathbf{e}^1$  of  $\mathbf{c}_2$  from the *a posteriori* probability by excluding  $\mathbf{a}(i)$ . The extrinsic information then serves as the *a priori* information to JUD in (20).

From the above decoding procedure, we can regard RDJD as a serial concatenated code, where soft information is serially updated between two constituent decoders JUD and RUD. Notably, the proposed rate-diverse GMAC outperforms SIC when two channel gains are even near-balanced and balanced. This is due to the fact that two users adopt code rates of large difference to distinguish the user messages. RUD uses a residual parity-check matrix for one user, which helps JUD to decode message for the other user with the common parity-check matrix.

#### IV. EXIT ANALYSIS FOR RATE-DIVERSE GMAC

In this section, we use an EXIT chart to illustrate the decoding behavior of RDJD by plotting the input/output relations of the constituent JUD and RUD decoders. This also provides an insight for rate allocation of GMAC with diverse channel conditions.

Recall that the inputs to JUD are the channel information and the extrinsic information from RUD, while the inputs to RUD is the extrinsic information from JUD. Note that only the extrinsic information for user 2 (i.e., the weak user) is iteratively updated between JUD and RUD. Let  $I_{U_A}$  denote the *a priori* mutual information between the coded bits and the input log-likelihood ratios (LLRs) of JUD for user 2; and  $I_{U_{E,m}}$  denote the mutual information between the coded bits

and the output LLRs of JUD for user  $m$ ,  $m = 1, 2$ . Similarly, let  $I_{RA}$  and  $I_{RE}$  denote the *a priori* mutual information and extrinsic mutual information of user 2 from RUD, respectively. The extrinsic output of RUD is the *a priori* information for JUD and vice versa. We measure the *a priori* mutual information between coded bit  $X$  and the LLR  $\xi$  by [33]

$$I_A = \frac{1}{2} \sum_{\mu \in \{+1, -1\}} \int_{-\infty}^{\infty} f_A(\xi|X = \mu) \times \log_2 \frac{2f_A(\xi|X = \mu)}{f_A(\xi|X = +1) + f_A(\xi|X = -1)} d\xi, \quad (25)$$

where  $f_A$  is the conditional probability density function. By simulated observations, we can model the *a priori* LLRs of the constituent decoders by an independent Gaussian random variable with variance  $\sigma_A^2$  and mean zero. Thus, we can compute  $I_{UA}$  and  $I_{RA}$  using

$$J(\sigma_A) = 1 - \int_{-\infty}^{\infty} \frac{\exp\left(-\frac{(\xi - \sigma_A^2/2)^2}{2\sigma_A^2}\right)}{\sqrt{2\pi\sigma_A^2}} \log_2 [1 + \exp(-\xi)] d\xi. \quad (26)$$

where  $J(\sigma_A)$  can be approximated by a polynomial [33]. Basically, an EXIT chart in RDJD includes two curves that characterize JUD and RUD, respectively. Each curve represents a relation between the *a priori* information and the extrinsic information. For each decoder, the mutual information between the coded bit  $X$  and the extrinsic LLR  $\xi$  can be measured by

$$I_E = \frac{1}{2} \sum_{\mu \in \{+1, -1\}} \int_{-\infty}^{\infty} f_E(\xi|X = \mu) \times \log_2 \frac{2f_E(\xi|X = \mu)}{f_E(\xi|X = +1) + f_E(\xi|X = -1)} d\xi, \quad (27)$$

where  $f_E(\xi|X = \mu)$  is the conditional PDF. For JUD,  $I_{UE,m}$  is defined as a function of  $I_{UA}$  and the channel information, i.e., SNR value, and is given by

$$I_{UE,m} = T_U(I_{UA}, SNR), \quad m = 1, 2, \quad (28)$$

where  $T_U$  represents JUD. Similarly, for RUD, we have

$$I_{RE} = T_R(I_{RA}), \quad (29)$$

where  $T_R$  represents RUD. Since the analytical treatments (28) and (29) for JUD and RUD are difficult to obtain, the distributions of  $f_E$  are most conveniently determined by Monte Carlo simulation (histogram measurements). Note that no Gaussian assumption is imposed on the distribution of the extrinsic outputs.

Given a received power  $|h_1|^2 + |h_2|^2 = 3.1$ , we show the decoding behavior of the RDJD under a sum rate  $R_1 + R_2 = 1.3$ . First, Fig. 6 shows the transfer characteristics  $I_{UE,m}$ ,  $m = 1, 2$ , from JUD at a SNR of 2.5 dB, where the x-axis and y-axis denote the *a priori* input  $I_{UA}$  and the extrinsic output  $I_{UE,m}$ , respectively. For all the rate pairs, we can see that  $I_{UE,2}$  from JUD are monotonically increasing in  $I_{UA}$ . It is reasonable that the reliability of user 2 becomes larger because  $I_{UE,2} = T_U(I_{UA}, SNR)$ . In particular,  $I_{UE,1}$  from JUD also increases with  $I_{UA}$  although  $I_{UA}$  is only related to the reliability of

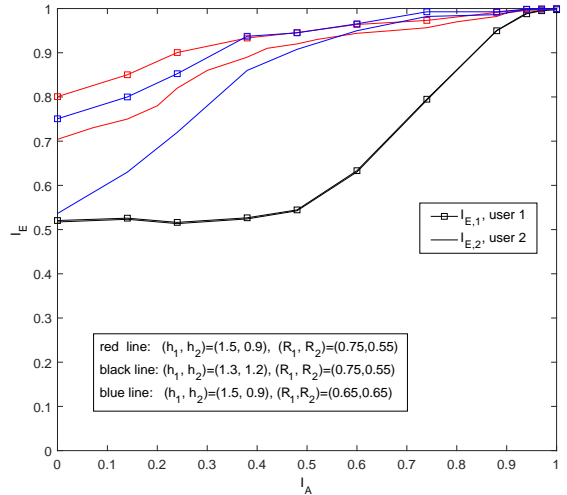


Fig. 6. Extrinsic information transfer characteristics of soft in/soft out for JUD at a SNR of 2.5 dB.

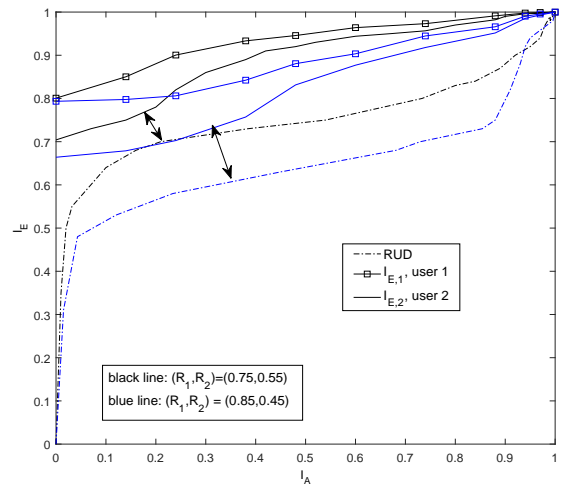


Fig. 7. EXIT chart with transfer characteristics of JUD and RUD at a SNR of 2.5 dB.

user 2. It is because JUD decodes the superimposed signal for the two user messages simultaneously, where the successful decoding of user 2 contributes to decoding convergence of user 1.

Second, Fig. 6 shows the effect of different channel conditions on RDJD. The extrinsic mutual information of both users with  $(h_1, h_2) = (1.5, 0.9)$  is much larger than that with  $(h_1, h_2) = (1.3, 1.2)$  given  $|h_1|^2 + |h_2|^2 = 3.1$ . Recall that JUD decodes four combinations, i.e., four superimposed symbols, of two user messages associated with  $h_1$  and  $h_2$ . As the values of  $h_1$  and  $h_2$  are close, some of the superimposed symbols become close, which leads to the reduced Euclidean distance between the symbols. In this case, the inter-user interference is equivalently severe and it is hard to distinguish one user from the other user.

Considering  $(h_1, h_2) = (1.5, 0.9)$  and  $R_1 + R_2 = 1.3$ , Fig. 6 shows that  $I_{UE,m}$  with rate pair  $(R_1, R_2) = (0.75, 0.55)$  is larger than that with  $(R_1, R_2) = (0.65, 0.65)$ ,  $m = 1, 2$ . We also see that  $I_{UE,1}$  has a larger initial value than  $I_{UE,2}$

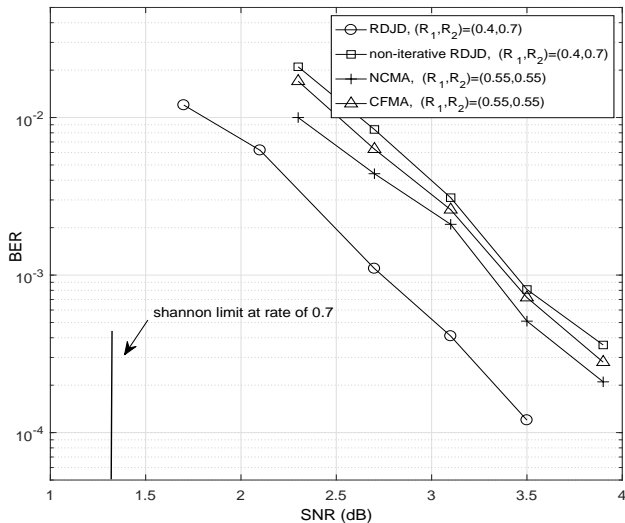


Fig. 8. BER performance of GMAC schemes at  $R_1 + R_2 = 1.10$ .

at the start point of  $I_{U_A} = 0$  due to the larger channel gain  $|h_1| > |h_2|$ . Accordingly,  $I_{U_{E,2}}$  has a gap from  $I_{U_{E,1}}$  during the iterations. However, as  $I_{U_A}$  for user 2 increases,  $I_{U_{E,2}}$  increases faster than  $I_{U_{E,1}}$  and the gap becomes narrower. In particular,  $I_{U_{E,2}}$  is almost the same as  $I_{U_{E,1}}$  when  $I_{U_A}$  becomes large enough, e.g.,  $I_{U_A} > 0.6$ .

Recall that JUD and RUD exchange extrinsic soft information iteratively. To account for the iterative nature, we also plot the EXIT curves of JUD and RUD in Fig. 7. The axes are swapped for transfer characteristics of the two decoders. We define the region between the two expected EXIT curves, one for the JUD and one for RUD, as the decoding tunnel. The figure plots the EXIT curves of RDJD with rate pairs  $(R_1, R_2) = (0.75, 0.55)$  and  $(R_1, R_2) = (0.85, 0.45)$ . At a SNR of 2.5 dB, the curves of JUD and RUD do not overlap for both cases. It means that RDJD can achieve a successful decoding with an arbitrarily small error probabilities for both cases. Moreover, we can see that the case with  $(R_1, R_2) = (0.85, 0.45)$  has a larger decoding tunnel than that with  $(R_1, R_2) = (0.75, 0.55)$ . Since a larger decoding tunnel implies a faster convergence rate and a lower decoding threshold, we deduce that the RDJD with  $(R_1, R_2) = (0.85, 0.45)$  converges faster and performs better than that with  $(R_1, R_2) = (0.75, 0.55)$ . Therefore, an optimized rate allocation is required to achieve the best performance.

## V. SIMULATION RESULT

In this section, we provide numerical simulations of the GMAC schemes and compare with the theoretical rate regions. For the theoretical rate regions, we evaluate theorem 1 with different discrete inputs. In our simulations, the total number of decoding iterations is set to 150. For fair comparison with iteratively decoded RDJD, the number of iterations between JUD and RUD is 5, and the number of channel decoding iterations is 30. We assume that a rate pair  $(R_1, R_2)$  is achieved for a given power and channel gains if the bit-error rate (BER) is below  $10^{-5}$  over 500 independent trials.

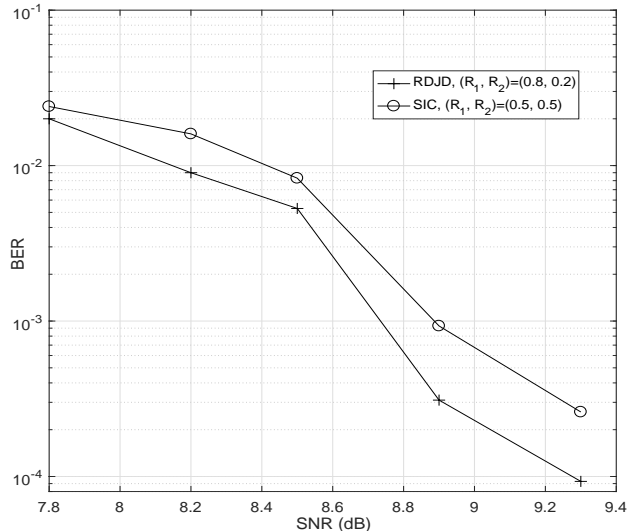


Fig. 9. The performance of RDJD and SIC under near power-balanced GMAC.

### A. Average Performance of different GMAC schemes

We compare the average BER performance of the two users in different GMAC schemes. Given a total transmission rate  $R_1 + R_2 = 1.1$ , we first consider a GMAC channel of  $(h_1, h_2) = (\sqrt{3}, 1.0)$ . For  $h_1 = \sqrt{3}$ , we employ a (273,191) LDPC code with a parity-check matrix  $\mathbf{H}_1$  of rate  $R_1 = 0.7$  [34]. For  $h_2 = 1.0$ , we generate a low-rate code  $\mathbf{H}_2$  of  $R_2 = 0.4$  by using our proposed RE method, which is achieved by appending 80 rows to  $\mathbf{H}_1$ . Each of the 80 rows has three ones placed in randomly selected positions. Fig. 8 shows that RDJD with iterative decoding has a large gain, about 0.8 dB, over RDJD without iterations. It is consistent with the EXIT result that shows iterations between JUD and RUD providing large gains. The figure also plots the BER of the conventional NCMA and CFMA, where the two users adopt the same parity-check matrix  $\mathbf{H}$  with  $R_1 = R_2 = 0.55$ . The matrix  $\mathbf{H}$  is generated by appending 40 rows to  $\mathbf{H}_1$  by the RE method. We see that iterative RDJD has significant gains, 0.6 dB and 0.7 dB, over NCMA and CFMA at a BER of  $3 \times 10^{-4}$ , respectively. Therefore, we can conclude that RUD can help to distinguish and decode two user messages in JUD iteratively since it provides independent information for the user 2. Moreover, we observe a large gap between AWGN capacity and the decoding performance of the existing GMAC schemes, and this gap can be greatly narrowed by the proposed RDJD.

Fig. 9 further compares the BER performance of the proposed scheme and the SIC scheme under near power-balanced GMAC. This scenario is highly desirable in practice since guaranteeing large received power differences between two users is not always possible [25]. With  $(h_1, h_2) = (1.0, 0.95)$ , two users in the proposed scheme is allocated with different coding rates  $(R_1, R_2) = (0.8, 0.2)$ , while the users in SIC scheme adopt the same rate  $(R_1, R_2) = (0.5, 0.5)$ . We can see from the figure that RDJD outperforms SIC by 0.4 dB at a BER of  $3 \times 10^{-4}$ . It is because the inter-user interference is large in near power-balanced scenarios. The effective SNR for



decoding the user messages is relatively small. The proposed scheme exploits a large residual matrix in the low-rate code, which provides a larger decoding capability than the SIC in the case of strong interference. In this way, we can decode one user message independently by RUD and use it as side information to decode the other user message in JUD.

### B. Performance of RDJD with different rate pairs

Next, we compare the BER performance of two users with different rate pairs over the channels with  $(h_1, h_2) = (1.5, 0.9)$ . Given LDPC codes of block length 5000 bits and a sum rate of  $R_1 + R_2 = 1.3$ , we consider three pairs of  $(R_1, R_2)$ , namely  $(0.75, 0.55)$ ,  $(0.85, 0.45)$ ,  $(0.95, 0.35)$ . The high-rate code with  $\mathbf{H}_1$  is the LDPC code optimized for point-to-point AWGN communications. The additional parity-check matrix appended to  $\mathbf{H}_1$  to form the low-rate code of  $\mathbf{H}_2$  is also optimized for point-to-point communications. Under iterative decoding, Fig. 10 shows that the system with  $(R_1, R_2) = (0.85, 0.45)$  outperforms that with  $(R_1, R_2) = (0.75, 0.55)$  by 0.7 dB at a BER of  $10^{-4}$ . It is because the inferior channel  $h_2 = 0.9$  requires a lower code rate to achieve successful decoding of user 2 in RUD. Moreover, the system with  $(R_1, R_2) = (0.85, 0.45)$  yields a gain of 0.5 dB over that with  $(R_1, R_2) = (0.95, 0.35)$  at a BER of  $10^{-4}$ . It is because that the common matrix  $\mathbf{H}_1$  of  $R_1 = 0.95$  provides less useful information than that with the lower rate  $R_1 = 0.85$  for the first user. The first user using the high-rate  $\mathbf{H}_1$  cannot be decoded successfully in JUD even with the reliable information of user 2 from RUD. The results suggest that there exists an optimal allocation of channel coding rates for the two users. In other words, given the channel gains and sum rate, we should consider proper rate allocation for the two users, which is associated with the common matrix and residual matrix for JUD and RUD, respectively.

Fig. 10 also shows that RDJD with  $(R_1, R_2) = (0.85, 0.45)$  achieves a significant gain of 1.0 dB over NCMA with the same rate  $(R_1, R_2) = (0.65, 0.65)$  at a BER of  $5 \times 10^{-4}$ . Moreover, it is interesting to note that two users have much different decoding performance in NCMA while they show similar performance, within only 0.1 dB difference, for RDJD. It is because the two users have the same rate in NCMA but with different channel initial reliability caused by different channel gains. In RDJD, iterative information exchange between JUD for the two users and RUD for one user offers a performance balance between the two users. Moreover, with long codewords, Fig. 11 demonstrates that the proposed rate-diverse GMAC with  $(R_1, R_2) = (0.85, 0.45)$  can attain the non-corner point of the dominant face of capacity region.

### C. Performance of RDJD with low rate transmission

We consider a low rate transmission with a sum rate  $R_1 + R_2 = 0.5$ ,  $(h_1, h_2) = (1.4, 0.8)$ , and a codeword length of 1024. NCMA adopts a rate pair  $(R_1, R_2) = (0.25, 0.25)$  for the two users, and the channel codes used are the protograph LDPC codes [35]. Fig. 12 shows that RDJD with  $(R_1, R_2) = (0.34, 0.16)$  outperforms that with  $(R_1, R_2) = (0.3, 0.2)$  by 0.3 dB at a BER of  $4 \times 10^{-4}$ . For RDJD, the parity-check

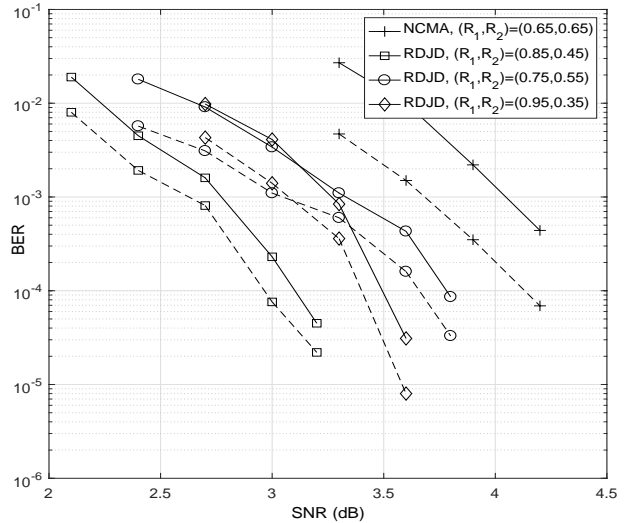


Fig. 10. BER performance of RDJD and NCMA at  $R_1 + R_2 = 1.3$ .

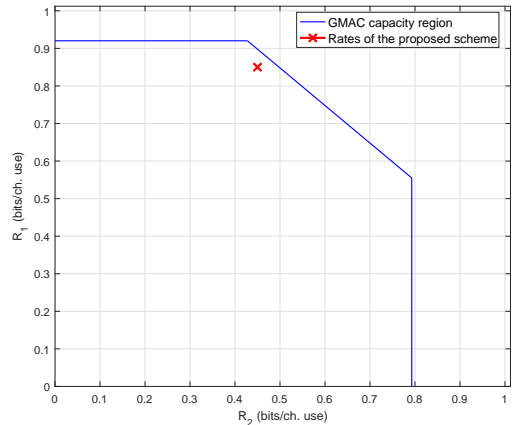


Fig. 11. Capacity region and rate pair of the proposed system.

matrices  $\mathbf{H}_1$  of  $R_1$  and  $\mathbf{H}_2$  of  $R_2$  are generated from  $\mathbf{H}$  by RC method and RE method, respectively. We can see that the RDJD with rate pair  $(R_1, R_2) = (0.34, 0.16)$  achieves a gain of 0.5 dB over non-iterative RDJD. The gains are less than that in the case with  $R_1 + R_2 = 1.25$ . It is because in the low rate transmission, both the parity-check matrices  $\mathbf{H}_1$  and  $\mathbf{H}_2$  are large. Thus, the additional decoding capability provided by  $\mathbf{H}_a$  in  $\mathbf{H}_2$  seems relatively low and has less effect on decoding both users' messages. However, the figure shows that the gain of RDJD over NCMA is still large, up to 0.8 dB, which is in part due to that JUD can yield a larger gain over XOR-CD at low rate than high rate.

### D. Performance of nonbinary channel-coded GMAC with 4PAM

Fig. 13 shows the symbol error rate (SER) of GMAC schemes with 4PAM modulation and nonbinary LDPC coding over the integer ring  $\mathbb{Z}_4$ . Regular LDPC codes with codeword length of 600 symbols are used. The non-zero entries of the parity-check matrix are multiplicative invertible elements (non-zero divisors), i.e.,  $\{1, 3\}$ , randomly selected from  $\mathbb{Z}_4$ . In

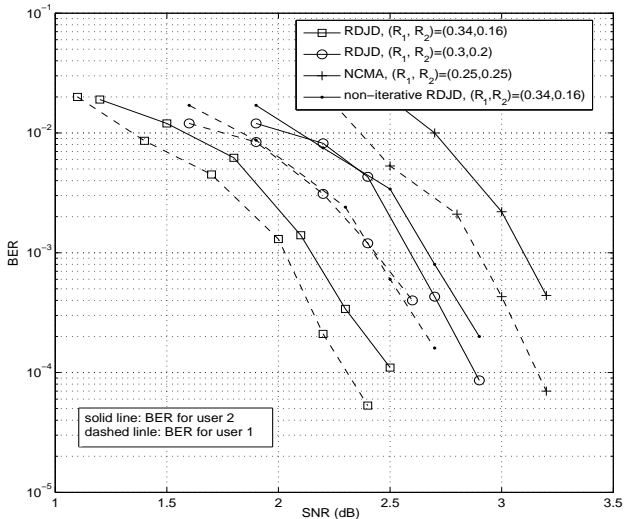


Fig. 12. BER performance of RDJD with different rate pairs at  $R_1 + R_2 = 0.5$ .

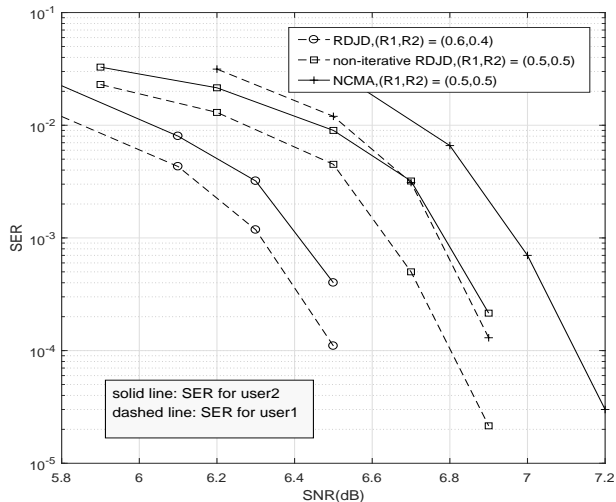


Fig. 13. SER performance of nonbinary channel-coded GMAC schemes with 4PAM over  $\mathbb{Z}_4$  at  $R_1 + R_2 = 1$ .

this scenario, JUD in RDJD is the generalized nonbinary SPA (G-SPA) proposed in [37], [38], and RUD is the conventional nonbinary SPA decoding. Similarly, XOR-CD in CMFA and NCMA is the network-coding-based channel decoding (NC-CD) that performs symbol-by-symbol NC mapping prior to channel decoding. Moreover, as in (7), NC-CD attempts to decode NC codeword with all possible coefficients, where  $(a_1, a_2)$  are limited to non-zero divisor in  $\mathbb{Z}_4$ ,  $(a_1, a_2) \in \{(1, 3), (1, 3), (3, 1), (3, 3)\}$ . Fig. 13 plots the SER results for  $(h_1, h_2) = (1.0, 0.8)$  and  $R_1 + R_2 = 1.0$ . We see that RDJD with  $(R_1, R_2) = (0.6, 0.4)$  has a performance gain of 0.5 dB over NCMA in nonbinary channel-coded cases, while non-iterative RDJD with  $(R_1, R_2) = (0.5, 0.5)$  slightly outperforms NCMA by 0.1 dB.

## VI. CONCLUSIONS

In this paper, we proposed a rate-diverse GMAC system that allows users to adopt different channel coding rate under dif-

ferent channel conditions. In the GMAC system, we proposed two channel code design methods for the two users such that the users with a good channel and an inferior channel employ the channel codes of a high code rate and a low code rate, respectively. Moreover, the two channel codes have some rows in their parity-check matrices identical. We then proposed an iterative RDJD as a serial concatenated decoder that consists of JUD and RUD as two constituent codes. The JUD decodes both user messages within the common parity-check matrix, and RUD provides independent information for the inferior channel user protected by the residual parity-check matrix. Moreover, we used the EXIT chart to show the decoding gain from the iterative decoding between JUR and RUD, and characterized the properties of different rate allocations for the two users.

To verify the EXIT analysis, we also studied the BER performance of the proposed system when LDPC channel codes were adopted. Our simulation showed that the iterative RDJD achieved a large gain over the conventional NCMA and CFMA schemes for both high rate and low rate transmissions. In particular, this gain could be more than 1 dB at relatively high rate cases. Moreover, we found that there existed an optimal rate allocation to obtain the best decoding performance for the two users given a constant sum rate. It suggested that the redundancy for JUD and RUD should be optimized to achieve decoding convergence according to different channels in GMAC.

## VII. APPENDIX A

• *Output Message of Variable Nodes.* Assume that the variable node  $\mathbf{v}$  is connected to two check nodes and channel initial message. Given the two input messages  $\mathbf{p} = [p^0, p^1, p^2, p^3]$  of the initial message and  $\mathbf{p}(1) = [p^0(1), p^1(1), p^2(1), p^3(1)]$  from the first check node, the outgoing probability message to the second check node, denoted by  $\mathbf{v}_{\rightarrow 2} = [v^0(2), v^1(2), v^2(2), v^3(2)]$ , where  $v^o(2)$  denotes the probability of  $\mathbf{v} = o$ , is given by

$$\begin{aligned} v^o(2) &= \Pr(\mathbf{v} = o | \mathbf{p}, \mathbf{p}(1)) = \frac{\Pr\{\mathbf{p}, \mathbf{p}(1) | \mathbf{v} = o\} \Pr\{\mathbf{v} = o\}}{\Pr\{\mathbf{p}, \mathbf{p}(1)\}} \\ &= \frac{\Pr\{\mathbf{v} = o | \mathbf{p}\} \Pr\{\mathbf{v} = o | \mathbf{p}(1)\} \Pr\{\mathbf{p}\} \Pr\{\mathbf{p}(1)\}}{\mathbf{v}\{\mathbf{v} = o\} \Pr\{\mathbf{p}, \mathbf{p}(1)\}} \\ &= \beta p^o p^o(1). \end{aligned} \quad (30)$$

Then, the output message is

$$\mathbf{v}_{\rightarrow 2} = \text{VAR}(\mathbf{p}, \mathbf{p}(1)). \quad (31)$$

• *Output Message of Check Nodes.* Suppose that a check node  $\mathbf{t}$  is connected to three variable nodes. We use  $\mathbf{q}(1) = [q^0(1), q^1(1), q^2(1), q^3(1)]$  and  $\mathbf{q}(2) = [q^0(2), q^1(2), q^2(2), q^3(2)]$  to denote the incoming messages from the variable nodes  $\mathbf{v}(1)$  and  $\mathbf{v}(2)$ , respectively. Let  $\mathbf{q} = [q^0, q^1, q^2, q^3]$  denote the probability of the coded bit  $\mathbf{v}$  from  $\mathbf{v}(1)$  and  $\mathbf{v}(2)$ , where  $q^o$  denotes the probability of  $\mathbf{v} = o$ . We calculate message  $\mathbf{q}$  based on  $\mathbf{q}(1)$  and  $\mathbf{q}(2)$ , with  $q^o$  being

$$q^o = \Pr(\mathbf{v} = o | \mathbf{q}(1), \mathbf{q}(2)) = \sum_{\substack{\varphi(m, n) = o, \\ m, n \in \Delta}} q^m(1) q^n(2), \quad (32)$$

where  $\varphi(m, n) = o$ , the bit-wise parity-check function of JUD, will be defined in (34), according to the LDPC encoding as below.

For the  $k$ th user, the check node  $\mathbf{t}$  is connected to three variable nodes  $\mathbf{v}_k(1)$ ,  $\mathbf{v}_k(2)$ , and  $\mathbf{v}_k(3)$ , satisfying

$$\mathbf{c}_k(1) \oplus \mathbf{c}_k(2) \oplus \mathbf{c}_k(3) = 0, \quad (33)$$

where  $k = 1, 2$ . Thus, the encoding of JUD also satisfies the same requirement. Suppose that three joint bit vectors corresponding to three variable nodes are  $\mathbf{c}_{1,2}(1) = [\mathbf{c}_1(1), \mathbf{c}_2(1)]$ ,  $\mathbf{c}_{1,2}(2) = [\mathbf{c}_1(2), \mathbf{c}_2(2)]$ , and  $\mathbf{c}_{1,2}(3) = [\mathbf{c}_1(3), \mathbf{c}_2(3)]$ , respectively. Moreover,  $m$ ,  $n$  and  $o$  are used to represent the decimal values of the three vectors, i.e.,  $m = \eta(\mathbf{c}_{1,2}(1))$ ,  $n = \eta(\mathbf{c}_{1,2}(2))$ , and  $o = \eta(\mathbf{c}_{1,2}(3))$ . Thus, with respect to (33), given a value of  $o$ , we define  $\varphi(m, n) = o$  in (32) as

$$\eta_k^{-1}(m) \oplus \eta_k^{-1}(n) = \eta_k^{-1}(o), \quad k = 1, 2. \quad (34)$$

As defined before,  $\eta_k^{-1}(m)$  is the  $k$ th bit of the bit vector converted from a decimal value  $m$ . Finally, the output message of  $\mathbf{t}$  is

$$\mathbf{t}_{\rightarrow 3} = \text{CHK}(\mathbf{q}(1), \mathbf{q}(2)). \quad (35)$$

#### REFERENCES

- [1] T. S. Han and K. Kobayashi, "A new achievable rate region for the interference channel," *IEEE Trans. Inf. Theory*, vol. 27, no. 1, pp. 49–60, 1981.
- [2] S. Verdú, *Multuser Detection*. Cambridge, U.K.: Cambridge Univ. Press, 1998.
- [3] Z. Ding, Z. Yang, P. Fan, and H. Poor, "On the performance of nonorthogonal multiple access in 5G systems with randomly deployed users," *IEEE Signal Process. Lett.*, vol. 21, no. 12, pp. 1501–1505, Dec. 2014.
- [4] B. Rimoldi and R. Urbanke, "A rate-splitting approach to the Gaussian multiple-access channel," *IEEE Trans. Inf. Theory*, vol. 42, no. 2, pp. 364–375, 1996.
- [5] A. J. Grant, B. Rimoldi, R. L. Urbanke, and P. A. Whiting, "Rate-splitting multiple access for discrete memoryless channels," *IEEE Trans. Inf. Theory*, vol. 47, no. 3, pp. 873–890, 2001.
- [6] J. Kelif, J. Gorce and A. Gati, "Performance and energy in green superposition coding wireless networks: an analytical model," in *GLOBECOM 2017*, Singapore, 2017, pp. 1-6.
- [7] S. Vanka, S. Srinivasa, Z. Gong, P. Vizi, K. Stamatiou, and M. Haenggi, "Superposition coding strategies: design and experimental evaluation," *IEEE Trans. Wireless Commun.*, vol. 11, no. 7, pp. 2628–2639, 2012.
- [8] S. M. R. Islam, N. Avazov, O. A. Dobre, and K.-S. Kwak, "Power-domain non-orthogonal multiple access (NOMA) in 5G systems: potentials and challenges," *IEEE Commun. Surveys Tuts.*, vol. 19, no. 2, pp. 721–742, 2nd Quart., 2016.
- [9] A. Benjebbour, Y. Saito, Y. Kishiyama, A. Li, A. Harada, and T. Nakamura, "Concept and practical considerations of non-orthogonal multiple access (NOMA) for future radio access," in *Proc. ISAPCS*, Nov. 2013, pp. 770–774.
- [10] R. Etkin, D. N. C. Tse, and H. Wang, "Gaussian interference channel capacity to within one bit," *IEEE Trans. Inf. Theory*, vol. 54, no. 12, pp. 5534–5562, Dec. 2008.
- [11] B. Bandemer, A. El Gamal, and Y.-H. Kim, "Simultaneous nonunique decoding is rate-optimal," in *Proc. 50th Ann. Allerton Conf. Comm. Control Comput.*, Monticello, IL, Oct. 2012.
- [12] H.-F. Chong, M. Motani, H. K. Garg, and H. El Gamal, "On the Han-Kobayashi region for the interference channel," *IEEE Trans. Inf. Theory*, vol. 54, no. 7, pp. 3188–3195, Jul. 2008.
- [13] S. Chen, B. Ren, Q. Gao, S. Kang, S. Sun, and K. Niu, "Pattern division multiple access (PDMA)—A novel non-orthogonal multiple access for 5G radio networks," *IEEE Trans. Veh. Technol.*, vol. 66, no. 4, pp. 3185–3196, Apr. 2017.
- [14] Z. Yuan, G. Yu, W. Li, Y. Yuan, X. Wang, and J. Xu, "Multi-user shared access for Internet of Things," in *Proc. IEEE VTC Spring*, May 2016, pp. 1–5.
- [15] T. Cover, "Broadcast channels," *IEEE Trans. Inf. Theory*, vol. 18, no. 1, pp. 2–14, Jan 1972.
- [16] N. I. Miridakis and D. D. Vergados, "A survey on the successive interference cancellation performance for single-antenna and multiple-antenna OFDM systems," *IEEE Commun. Surveys Tutorials*, vol. 15, no. 1, pp. 312–335, Feb. 2013.
- [17] A. Roumy and D. Declercq, "Characterization and optimization of LDPC codes for the 2-user Gaussian multiple access channel," *EURASIP J. Wireless Commun. Netw.*, vol. 2007, Art. no. 074890, 2007.
- [18] A. Balatsoukas-Stimming and A. P. Liavas, "Design of LDPC codes for the unequal power two-user Gaussian multiple access channel," *IEEE Wireless Commun. Lett.*, vol. 7, no. 5, pp. 868–871, Oct. 2018.
- [19] S. Sharifi, A. K. Tanc and T. M. Duman, "LDPC code design for the two-user Gaussian multiple access channel," *IEEE Trans. Wireless Commun.*, vol. 15, no. 4, pp. 2833–2844, April 2016.
- [20] J. Du, L. Zhou, L. Yang, S. Peng, and J. Yuan, "A new LDPC coded scheme for two-User Gaussian multiple access channels," *IEEE Commun. Lett.*, vol. 22, no. 1, pp. 21–24, 2018.
- [21] L. Lu, L. You, and S. C. Liew, "Network-coded multiple access," *IEEE Trans. Mobile Comput.*, vol. 13, no. 12, pp. 2853–2869, Dec. 2014.
- [22] S. Zhang and S. C. Liew, "Channel coding and decoding in a relay system operated with physical-layer network coding," *IEEE J. Sel. Areas Commun.*, vol. 27, no. 5, pp. 788–796, Oct. 2009.
- [23] L. You, S. C. Liew and L. Lu, "Network-coded multiple access II: toward real-time operation with improved performance," *IEEE J. Sel. Areas Commun.*, vol. 33, no. 2, pp. 264–280, Feb. 2015.
- [24] H. Pan, L. Lu and S. C. Liew, "Network-coded multiple access with high-order modulations," *IEEE Trans. Veh. Technol.*, vol. 66, no. 11, pp. 9776–9792, Nov. 2017.
- [25] H. Pan, L. Lu, and S. C. Liew, "Practical power-balanced non-orthogonal multiple access," *IEEE J. Sel. Areas Commun.*, vol. 35, no. 10, pp. 2312–2327, Oct. 2017.
- [26] H. Pan, S. C. Liew, J. Liang, Y. Shao and L. Lu, "Network-coded multiple access on unmanned aerial vehicle," *IEEE J. Sel. Areas Commun.*, vol. 36, no. 9, pp. 2071–2086, Sept. 2018.
- [27] B. Nazer and M. Gastpar, "Compute-and-forward: Harnessing interference through structured codes," *IEEE Trans. Inf. Theory*, vol. 57, no. 10, pp. 6463–6486, Oct. 2011.
- [28] T. Wang, S. C. Liew and L. Shi, "Optimal rate-diverse wireless network coding," *IEEE Trans. Commun.*, vol. 65, no. 6, pp. 2411–2426, June 2017.
- [29] J. Zhu and M. Gastpar, "Gaussian multiple access via compute-and-forward," *IEEE Trans. Inf. Theory*, vol. 63, pp. 2678–2695, May 2017.
- [30] J. Zhu and M. Gastpar, "On lattice codes for Gaussian interference channels," *2015 IEEE International Symposium on Information Theory (ISIT)*, Jun. 2015, pp. 2066–2070.
- [31] S. H. Lim, C. Feng, A. Pastore, B. Nazer, and M. Gastpar, "A joint typicality approach to algebraic network information theory," *ArXiv eprints*, Jun. 2016, preprint available at <http://arxiv.org/abs/1606.09548>.
- [32] E. Sula, J. Zhu, A. Pastore, S. H. Lim and M. Gastpar, "Compute-forward multiple access (CFMA): practical implementations," *IEEE Trans. Wireless Commun.*, vol. 67, no. 2, pp. 1133–1147, Feb. 2019.
- [33] S. ten Brink, "Convergence behavior of iteratively decoded parallel concatenated codes," *IEEE Trans. Commun.*, vol. 49, no. 10, pp. 1727–1737, Oct. 2001.
- [34] Y. Kou, S. Lin and M. P. C. Fossorier, "Low-density parity-check codes based on finite geometries: a rediscovery and new results," *Trans. Inf. Theory*, vol. 47, no. 7, pp. 2711–2736, Nov. 2001.
- [35] Y. Fang, G. Bi, Y. L. Guan and F. C. M. Lau, "A survey on protograph LDPC codes and their applications," *IEEE Commun. Surveys Tuts.*, vol. 17, no. 4, pp. 1989–2016, Fourthquarter 2015.
- [36] T. M. Cover and J. A. Thomas, *Elements of Information Theory*, 2nd ed. New York: Wiley, 2006.
- [37] P. Chen, L. Shi, S. C. Liew, Y. Fang and K. Cai, "Channel decoding for nonbinary physical-layer network coding in two-way relay systems," *IEEE Trans. Veh. Technol.*, vol. 68, no. 1, pp. 628–640, Jan. 2019.
- [38] P. Chen, S. C. Liew, and L. Shi, "Bandwidth-efficient coded modulation scheme for physical-layer network coding with high-order modulations," *IEEE Trans. Commun.*, vol. 65, no. 1, pp. 147–160, Jan. 2017.